Materials Chemistry and Physics 149-150 (2015) 582–586

Contents lists available at ScienceDirect

Materials Chemistry and Physics

journal homepage: www.elsevier.com/locate/matchemphys

Gold nanoparticles: BSA (Bovine Serum Albumin) coating and X-ray irradiation produce variable-spectrum photoluminescence

Kuo-Hao Lee [a, b], Sheng-Feng Lai [b, c], Yan-Cheng Lin [a], Wu-Ching Chou [a], Edwin B.L. Ong [b], Hui-Ru Tan [d], Eng Soon Tok [e], C.S. Yang [f], G. Margaritondo [g], Y. Hwu [b, h, i, *]

[a] Department of Electrophysics, National Chiao Tung University, Hsinchu, Taiwan
[b] Institute of Physics, Academia Sinica, Taipei 115, Taiwan
[c] Department of Engineering Science, National Cheng Kung University, Tainan 701, Taiwan
[d] Institute of Materials Research and Engineering, 3 Research Link, 117602, Singapore
[e] Physics Department, National University of Singapore, 117542, Singapore
[f] Center for Nanomedicine, National Health Research Institutes, Miaoli 350, Taiwan
[g] Ecole Polytechnique Fédérale de Lausanne (EPFL), CH-1015 Lausanne, Switzerland
[h] Advanced Optoelectronic Technology Center, National Cheng Kung University, Tainan 701, Taiwan
[i] Institute of Optoelectronic Sciences, National Taiwan Ocean University, Keelung 202, Taiwan

HIGHLIGHTS

- Gold nanoparticles (Au NPs) coated with Bovine Serum Albumin (BSA) are synthesized by x-ray irradiation.
- BSA coated AuNPs with ~1 nm size show strong photoluminescence in red by UV excitation.
- The blue photoluminescence of BSA increase with x-ray irradiation.
- Increase x-ray irradiation time during the synthesis shift the color of the colloid from red to blue.

ARTICLE INFO

Article history:
Received 28 June 2014
Received in revised form
10 October 2014
Accepted 1 November 2014
Available online 14 November 2014

Keywords:
Nanostructures
Luminescence
Irradiation effect
Visible and ultraviolet spectrometers

ABSTRACT

We show that by using different x-ray irradiation times of BSA-coated Au nanoparticles (NPs) we can change their ultraviolet-stimulated photoluminescence and shift the spectral weight over the visible spectral range. This is due to the interplay of two emission bands, one due to BSA and the other related to gold. The emission properties did not change with time over a period of several months.

Protein-stabilized photoluminescent metal nanocluster promises applications such as luminescence tagging, imaging, medical diagnostics, multiplexing and biosensors [1–5] taking advantage of their small particle size, biocompatibility and the stable emission in biological environments [6–8]. Protein-nanoparticle interaction also induces other interesting properties [9–11]. Bovine serum albumin (BSA), a commonly studied protein and is extensively used for biochemical applications, was used as a reducing agent and a template to prepared Au nanoparticles at physiological temperature with strong red photoluminescence [12].

We discovered that BSA coated and x-ray-irradiated Au NPs photoluminescence in the visible. Furthermore, the spectral weight of the emission changes from red to blue as the irradiation time increases. The details of the mechanism are not all clear but our experiments establish some firm points. The color change is due to the interplay of two spectral emission bands, one in the blue due to BSA and the second in the red, which is linked to gold. As the irradiation continues, the first band becomes more intense and the second is progressively quenched. Practically speaking, these phenomena could be exploited to fabricate stable NPs with the desired

* Corresponding author. Institute of Physics, Academia Sinica, Taipei 115, Taiwan.
E-mail address: phhwu@sinica.edu.tw (Y. Hwu).

http://dx.doi.org/10.1016/j.matchemphys.2014.11.009
0254-0584/

photoluminescence color with simple changes of x-ray irradiation time.

Our experiments were motivated by recent results on photoluminescence from MUA-coated (MUA = 11-mercaptoundecanoic acid) Au NPs [13–15] synthesized by X-ray irradiation. In that case, however, we did not observe any color change. Photoluminescence is known to occur only for very small (<2 nm diameter) NPs [4,16–21]. Likewise, in our case only the smallest BSA-coated Au NPs exhibit photoluminescence – with the added feature of irradiation-time-dependent color: we are able to tune the color of the colloidal solution from red to blue by simply increase the x-ray irradiation time.

Prior to the discovery of photoluminescence from small MUA-coated Au NPs, this line of experiments demonstrated that x-ray irradiation produces very stable NPs of different metals [22–26] and different sizes and shapes [27–30] all with excellent shelf life. Fast reduction of metal ions, a complete reduction is achieved within milliseconds, by intense x-ray irradiation and subsequently coating with MUA, PEG (poly(ethylene glycol)) and other thiol-based molecules enabled us to accurately control the NP size and to narrow the size distribution [31–33]. Such features were also observed in the present experiments on BSA-coated Au NPs.

The photoluminescence properties of MUA and BSA coated Au NPs additionally expand the potential applications of such systems [6–8]. We investigated them for BSA-coated particles emission spectroscopy and absorption spectroscopy. The emission spectra – see Fig. 1 – directly show the cause of the color change: the interplay of the "blue" band peaked at 470–480 nm whose intensity increases with the irradiation time, and of the "red" band at 670–700 nm, which is progressively quenched.

The intrinsic blue photoluminescence of BSA was reported at different emission wavelength under different chemical conditions [34,35]. Fig. 2 shows indeed emission spectra from a solution of pure BSA: we see the same band and similar intensity increase with the x-ray irradiation time, without the "red" band. This contradict to previous finding using γ-ray irradiation which quenched the blue emission [34,35]. Ionization radiations generally change the protein structure by breaking the covalent bonds causing polypeptide chain disruption. Oxygen radials generated by radiation could modify primary structure of proteins and affects their secondary and tertiary structure [36,37]. The exact modification of the BSA protein structure due to x-ray irradiation is not clear, but we note that the peak of blue emission stay fixed at 470–480 nm. The identification of the "red" band is slightly more complex and is discussed later.

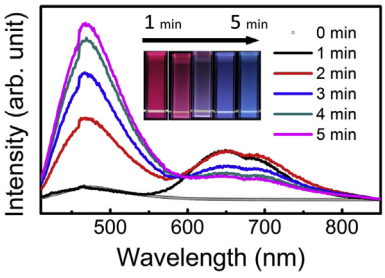

Fig. 1. Photoluminescence (produced by 400 nm wavelength excitation) spectra of BSA-Au NPs. The precursor solution had an R-value of 3.2. The curves correspond to different x-ray irradiation times. The inset shows photograph of the photoluminescence after x-ray irradiation for 1, 2, 3, 4 and 5 min: note the striking change in color, caused by the interplay of the "red" and "blue" bands. (For interpretation of the references to color in this figure legend, the reader is referred to the web version of this article.)

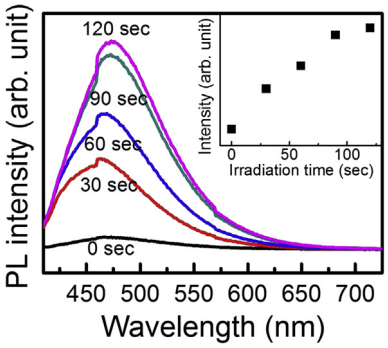

Fig. 2. Photoluminescence (again for 400 nm excitation) spectra of BSA alone, exhibiting only the "blue" band. Inset: Increase with irradiation time of the fluorescence peak height. (For interpretation of the references to color in this figure legend, the reader is referred to the web version of this article.)

The experimental procedure started with a precursor solution, obtained by mixing 0.5 mL of 10 mM $HAuCl_4 \cdot 3H_2O$ (Sigma–Aldrich) with different BSA (also from Sigma–Aldrich) amounts. The solution volume was then increased to 9.5 mL by adding distilled deionized (dd) water. After 2 min, we added 0.5 mL of 1 M NaOH (also from Sigma–Aldrich). Since one BSA molecule contains 40 S atoms [38,39], we can define the S-to-Au molar ratio (R) as:

$$R = \frac{\text{Final molar concentration of BSA}}{\text{Final molar concentration of Au}} \times 40$$

We then placed the solution in polypropylene conical tubes and, after stirring, we irradiated it with hard x-rays from the BL01A beamline of the NSRRC (National Synchrotron Radiation Research Center) in Hsinchu, Taiwan. The NSRRC storage ring was running at a constant electron current of 300 mA. The x-ray photon energy ranged from 8 to 15 keV and was centered at ~12 keV; the delivered dose rate was ~4.7×10^5 Gy s^{-1} [40].

After irradiation, we purified the solution removing residual ions and impurities by dialysis (with cellulose membrane, molecular weight cutoff (MWCO) 10,000) against dd water for at least 2 days, with the water being changed periodically. To study photoluminescence from pure BSA, we used the same procedure but without $HAuCl_4 \cdot 3H_2O$ in the precursor solution.

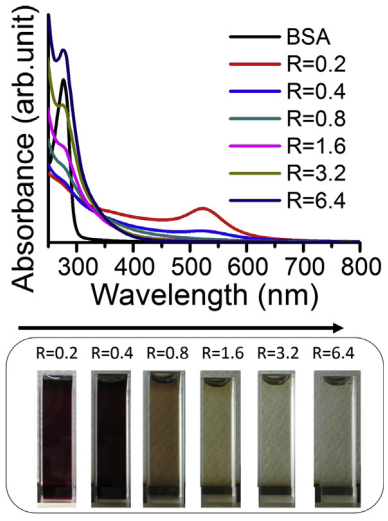

Fig. 3. UV–visible spectra of colloidal gold nanoparticles synthesized in the presence of BSA with different R-values, after a short (120 s) x-ray irradiation.

The irradiated solutions were characterized with different techniques: UV–visible spectra were acquired over the 200–800 nm range using a DU800 Spectrophotometer (Beckman Coulter, USA) with a quartz cuvette. We took transmission electron microscopy (TEM) images of the dried solution using a JEOL JEM-2100F system with a 4096 × 4096 CCD (Gatan, UltraScan 4000) operated at 200 kV. The dried solution was obtained at 40 °C after placing a drop on a carbon-coated Cu grid. We also performed scanning transmission electron microscopy (STEM) analysis of <2 nm Au NPs in the HAADF (high angle annular dark field) mode using an FEI Titan 80–300 system.

Photoluminescence emission and excitation spectra were taken at room temperature with a Cary Eclipse spectrophotometer (Varian, USA). We excited the luminescence with a dye pulsed laser (377 nm/50 MHz) coupled to SPEX 1403 double-grating 0.85 m spectrometer and to a high-speed photomultiplier. The photoluminescence lifetime was measured also at room temperature at 300 K by a time-resolved photoluminescence (TRPL) system.

Our tests showed that, as for Au-NPs coated with other thiol-based molecules, the R-value controls the nanoparticle size. Indeed, as the R-value changed from 0.2 to 1.6, the solution color after irradiation changed from red to yellow, indicating a particle

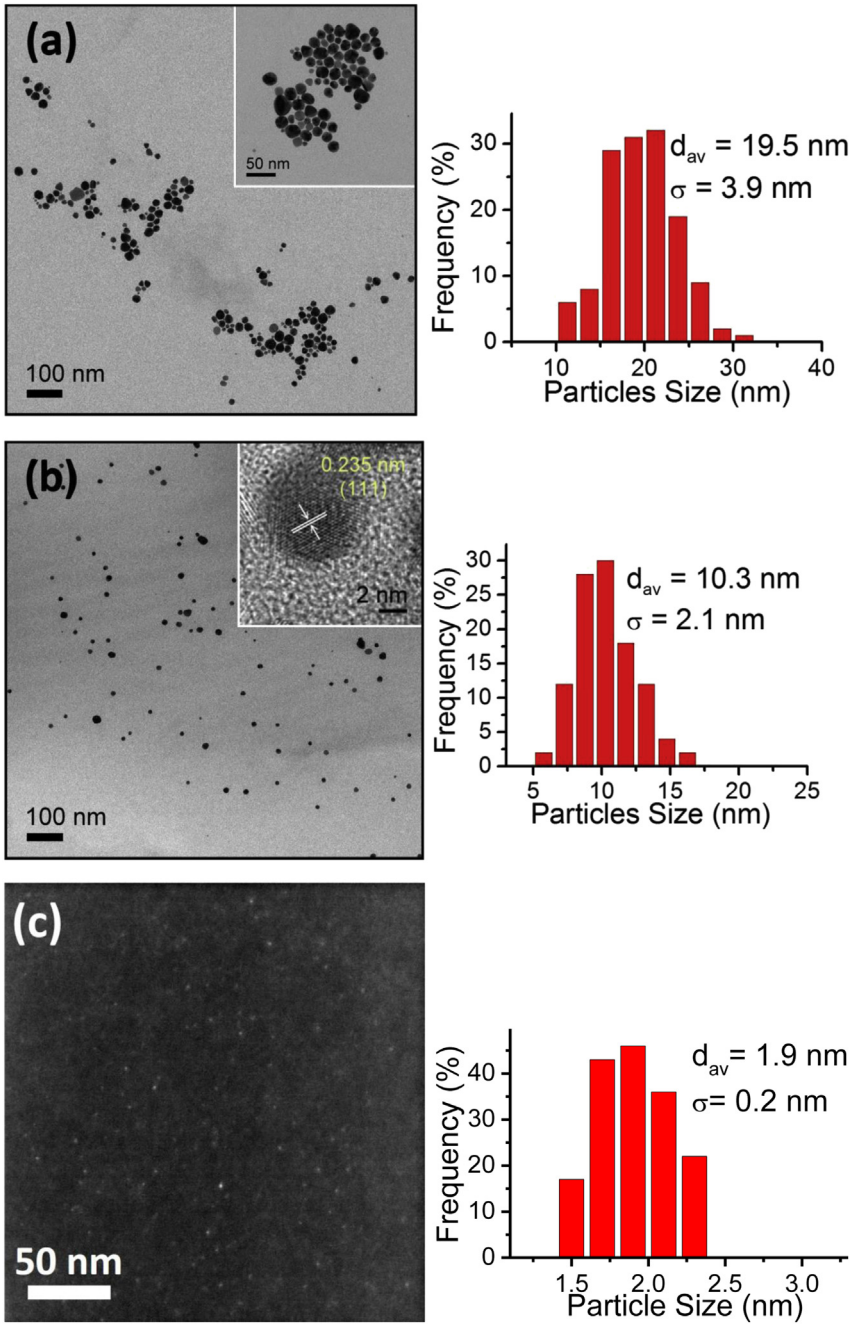

Fig. 4. TEM micrographs of Au NPs synthesized in the presence of BSA as for Fig. 3, for (a) R = 0.2, (b) R = 0.4 and (c) R = 3.2 (dark field image). On the bottom right, we see the size histogram corresponding to Fig. (c). Inset in (a): magnified portion of the same micrograph. Inset in (b): at high magnification, TEM reveals the lattice planes in a nanoparticle with Au(111) spacing, 0.235 nm.

size decrease. For R = 0.2 and after a short x-ray irradiation for 120 s, the UV–visible spectra (Fig. 3) exhibited a plasmon band at 522 nm, caused by the formation of Au nanoparticles. As R increased, the plasmon band first blue-shifted as expected for a decreasing particle size [41–43]. At R > 0.8, the particles became too small to host plasmons [44–46], the band disappeared and the solution became essentially transparent.

The UV–visible absorption, therefore, can only characterize the size of relatively large Au clusters produced by large R-values. For smaller R-values and clusters, we used high-resolution TEM – see Fig. 4 – to prove that the size keeps decreasing. However, for the smallest clusters we had to use dark-field STEM rather than bright-field TEM. The average particle size was 19.5 ± 3.9, 10.3 ± 2.1 and ~1.9 nm for R = 0.2, 0.4 and 3.2.

As already mentioned, the size decrease was essential to produce photoluminescence. In fact, as for MUA-Au NPs, no emission was detected from large particles corresponding to R-values below 3.2. As the average nanoparticle size reached ≈2 nm (the same value as for MUA-Au NPs), photoluminescence started to appear.

We now go back to the discussion of the two photoluminescence bands whose interplay produces the color change. Having clarified the nature of the "blue" band as due to BSA, we will concentrate our attention on the "red" band. To explore its nature, we measured the temperature dependence of the photoluminescence spectrum. Fig. 5 shows the results for a sample yielded by R = 3.2 precursor solution at room temperature. We clearly see that the "red" band actually includes two components, labeled as "band I" and "band II".

As shown in Fig. 6 (top), the two bands shift in opposite directions as the temperature increases. Such results are closely related to those of X. Wen et al. [47] on BSA-protected Au_{25} nanoclusters, so that we can adopt similar conclusions on the nature of the two red sub-bands. In essence, band I is attributed to a semiconductor-like emission from the core Au atoms in the cluster and band II is attributed instead to S–Au bonds.

The red shift of band I as the temperature increases is explained by the standard mechanisms affecting the semiconductor gap, notably electron–phonon interaction [48]. Similar to X. Wen et al. [47], we fitted the shift with temperature with the standard Varshni and O'Donnell–Chen equations [49,50] (see the latter case in Fig. 6, bottom). The similarity with the results of X. Wen et al. [47], however, is not absolute: the spectral positions of our peaks are somewhat different, and the cause of this difference is not yet clear.

As to the blue shift of band II, we concur with the conclusion of Ref. [47]. In essence, this shift is simply due to the increasing separation between adjacent atoms in the subnanostructures where the S–Au binds are located.

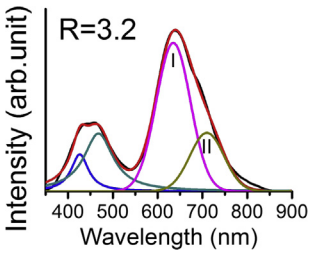

Fig. 5. The photoluminescence (PL) spectrum (black) for a sample yielded by an R = 3.2 precursor solution measured at room temperature. The "red" band can be represented by two Gaussian peaks ($R^2 > 0.99$), labeled as "band I" and "band II". The overall fit (red) includes decomposition of the "blue" band. (For interpretation of the references to color in this figure legend, the reader is referred to the web version of this article.)

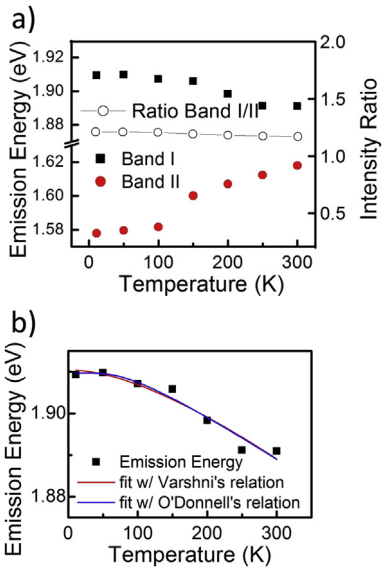

Fig. 6. The temperature-dependent photoluminescence spectra analysis for Fig. 6. (a) The photoluminescence spectra from 11 K to 300 K. (b) The emission peaks shift for "band I" and "band II" from 11 K to 300 K. (c) The peak shift fitting for "band I" by Varshni and O'Donnell–Chen equations.

Further experiments are underway to completely clarify the nature of the different photoluminescence spectral components – and possibly to identify mechanisms that could further increase the flexibility in controlling the color of the emission. These improvements will further enhance the potential application in area such as tumor markings for surgery and multicolor biomarkers. Even at this stage, however, we can conclude that the photoluminescence color from these nanosystems can be simply and reliably changed over the entire visible range by controlling the x-ray irradiation time. The potential for applications is quite clear.

Acknowledgments

Work supported by the National Science and Technology Program for Nanoscience and Nanotechnology, the Thematic Research Project of Academia Sinica, the Biomedical Nano-Imaging Core Facility at National Synchrotron Radiation Research Center (Taiwan), the Fonds National Suisse pour la Recherche Scientifique and the Center for Biomedical Imaging (CIBM, supported by the Louis-Jeantet and Leenards foundations).

References

[1] J. Xie, Y. Zheng, J.Y. Ying, Chem. Commun. 46 (2010) 961.
[2] C.C. Huang, Z. Yang, K.H. Lee, H.T. Chang, Angew. Chem. Int. Ed. 46 (2007) 6824.
[3] M.A.H. Muhammed, P.K. Verma, S.K. Pal, A. Retnakumari, M. Koyakutty, S. Nair, T. Pradeep, Chem-Eur. J. 16 (2010) 10103.
[4] D.M. Chevrier, A. Chatt, P. Zhang, J. Nanophot. 6 (2012) 064504.
[5] H. Kawasaki, K. Hamaguchi, I. Osaka, R. Arakawa, Adv. Funct. Mater. 21 (2011) 3508.
[6] J.P. Wilcoxon, J.E. Martin, F. Parsapour, B. Wiedenman, D.F. Kelley, J. Chem. Phys. 108 (1998) 9137.
[7] Z. Li, Q. Sun, Y. Zhu, B. Tan, Z.P. Xu, S.X. Dou, J. Mat. Chem. B 2 (2014) 2793.
[8] S. Hong-Tao, S. Yoshio, Sci. Technol. Adv. Mater. 15 (2014) 014205.
[9] T. Sen, K.K. Haldar, A. Patra, J. Phys. Chem. C. 112 (2008) 17945.
[10] T. Sen, S. Mandal, S. Haldar, K. Chattopadhyay, A. Patra, J. Phys. Chem. C. 115 (2011) 4037.
[11] B. Paramanik, A. Kundu, K. Chattopadhyay, A. Patra, RSC Adv. 4 (2014) 35059.
[12] J.P. Xie, Y.G. Zheng, J.Y. Ying, J. Am. Chem. Soc. 131 (2009) 888.
[13] S.F. Lai, C.C. Chien, W.C. Chen, H.H. Chen, Y.Y. Chen, C.L. Wang, Y. Hwu, C.S. Yang, C.Y. Chen, K.S. Liang, C. Petibois, H.R. Tan, E.S. Tok, G. Margaritondo, Biotechnol. Adv. 31 (2013) 362.

[14] S.F. Lai, C.C. Chien, W.C. Chen, Y.Y. Chen, C.H. Wang, Y. Hwu, C. Yang, G. Margaritondo, R. Soc, Chem. Adv. 2 (2012) 6185.
[15] C.C. Huang, H.Y. Liao, Y.C. Shiang, Z.H. Lin, Z. Yang, H.T. Chang, J. Mater. Chem. 19 (2009) 755.
[16] C.A. Lin, C.H. Lee, J.T. Hsieh, H.H. Wang, J.K. Li, J.L. Shen, W.H. Chan, H.I. Yeh, W.H. Chang, J. Med. Biol. Eng. 29 (2009) 276.
[17] N. Schaeffer, B. Tan, C. Dickinson, M.J. Rosseinsky, A. Laromain, D.W. McComb, M.M. Stevens, Y. Wang, L. Petit, C. Barentin, D.G. Spiller, A.I. Cooper, R. Levy, Chem. Commun. 14 (2008) 3986.
[18] T.P. Bigioni, R.L. Whetten, Ö. Dag, J. Phys. Chem. B 104 (2000) 6983.
[19] H. Duan, S. Nie, J. Am. Chem. Soc. 129 (2007) 2412.
[20] S.Y. Lin, N.T. Chen, S.P. Sum, L.W. Lo, C.S. Yang, Chem. Commun. 39 (2008) 4762.
[21] S.Y. Lin, N.T. Chen, S.P. Sun, J.C. Chang, Y.C. Wang, C.S. Yang, L.W. Lo, J. Am. Chem. Soc. 132 (2010) 8309.
[22] C.L. Wang, B.J. Hsao, S.F. Lai, W.C. Chen, H.H. Chen, Y.Y. Chen, C.C. Chien, X. Cai, I.M. Kempson, Y. Hwu, G. Margaritondo, Nanotechnology 22 (2011) 065605.
[23] C.H. Wang, C.J. Liu, C.L. Wang, C.C. Chien, Y. Hwu, R.S. Liu, C.S. Yang, J.H. Je, H.M. Lin, G. Margaritondo, Appl. Phys. A 97 (2009) 295.
[24] C.C. Kim, C.H. Wang, Y.C. Yang, Y. Hwu, S.K. Seol, Y.B. Kwon, C.H. Chen, H.W. Liou, H.M. Lin, G. Margaritondo, J.H. Je, Mater. Chem. Phys. 100 (2006) 292.
[25] Y.C. Yang, C.H. Wang, Y.K. Hwu, J.H. Je, Mater. Chem. Phys. 100 (2006) 72.
[26] C.H. Wang, T.E. Hua, C.C. Chien, Y.L. Yu, T.Y. Yang, C.J. Liu, W.H. Leng, Y. Hwu, Y.C. Yang, C.C. Kim, J.H. Je, C.H. Chen, H.M. Lin, G. Margaritondo, Mater. Chem. Phys. 106 (2007) 323.
[27] C.H. Wang, C.C. Chien, Y.L. Yu, C.J. Liu, C.F. Lee, C.H. Chen, Y. Hwu, C.S. Yang, J.H. Je, G. Margaritondo, J. Synchrotron Radiat. 14 (2007) 477.
[28] X. Cai, C.L. Wang, H.H. Chen, C.C. Chien, S.F. Lai, Y.Y. Chen, T.E. Hua, I.M. Kempson, Y. Hwu, C.S. Yang, G. Margaritondo, Nanotechnology 21 (2010) 335604.
[29] H.T. Tung, I.G. Chen, J.M. Song, M.G. Tsai, I.M. Kempson, G. Margaritondo, Y. Hwu, Nanoscale 5 (2013) 4706.
[30] H.T. Tung, I.G. Chen, I.M. Kempson, J.M. Song, Y.F. Liu, P.W. Chen, W.S. Hwang, Y. Hwu, ACS Appl. Mater. Interfaces 4 (2012) 5930.
[31] S.F. Lai, W.C. Chen, C.L. Wang, H.H. Chen, S.T. Chen, C.C. Chien, Y.Y. Chen, W.T. Hung, X.Q. Cai, E.R. Li, I.M. Kempson, Y. Hwu, C.S. Yang, E.S. Tok, H.R. Tan, M. Lin, G. Margaritondo, Langmuir 27 (2011) 8424.
[32] C.H. Wang, C.J. Liu, C.L. Wang, T.E. Hua, J.M. Obliosca, K. Lee, Y. Hwu, C.S. Yang, R.S. Liu, H.M. Lin, J.H. Je, G. Margaritondo, J. Phys. D. Appl. Phys. 41 (2008) 195301.
[33] X.Q. Cai, H.H. Chen, C.L. Wang, S.T. Chen, S.F. Lai, C.C. Chien, Y.Y. Chen, I.M. Kempson, Y. Hwu, C.S. Yang, G. Margaritondo, Anal. Bioanal. Chem. 401 (2011) 809.
[34] S. Moon, K.B. Song, Food Chem. 74 (2001) 479.
[35] M.H. Gaber, J. Biosci. Bioeng. 100 (2005) 203.
[36] K.J.A. Davies, J. Biol. Chem. 262 (1987) 9895.
[37] K.J.A. Davies, M.E. Delsignore, J. Biol. Chem. 262 (1987) 9908.
[38] M. Oblak, A. Prezelj, S. Pecar, T. Solmajer, Z Naturforsch C. 59 (2004) 880.
[39] C.L. Guo, J. Irudayaraj, Anal. Chem. 83 (2011) 2883.
[40] C.J. Liu, C.H. Wang, C.L. Wang, Y. Hwu, C.Y. Lin, G. Margaritondo, J. Synchrotron Radiat. 16 (2009) 395.
[41] S. Link, M.A. El-Sayed, J. Phys. Chem. B 103 (1999) 8410.
[42] M.J. Hostetler, J.E. Wingate, C.J. Zhong, J.E. Harris, R.W. Vachet, M.R. Clark, J.D. Londono, S.J. Green, J.J. Stokes, G.D. Wignall, G.L. Glish, M.D. Porter, N.D. Evans, R.W. Murray, Langmuir 14 (1998) 17.
[43] U. Kreibig, K. Fauth, M. Quinten, D. Schonauer, Z. Phys. D–Atom. Mol. Cl. 12 (1989) 505.
[44] S. Link, M.A. El-Sayed, Int. Rev. Phys. Chem. 19 (2000) 409.
[45] M.M. Alvarez, J.T. Khoury, T.G. Schaaff, M.N. Shafigullin, I. Vezmar, R.L. Whetten, J. Phys. Chem. B 101 (1997) 3706.
[46] Y.G. Kim, S.K. Oh, R.M. Crooks, Chem. Mater. 16 (2004) 167.
[47] X. Wen, P. Yu, Y.R. Toh, J. Tang, J. Phys. Chem. C. 116 (2012) 11830.
[48] A. Narayanaswamy, L.F. Feiner, A. Meijerink, P.J. van der Zaag, ACS Nano 3 (2009) 2539.
[49] Y.P. Varshni, Physica 34 (1967) 149.
[50] K.P. O'Donnell, X. Chen, Appl. Phys. Lett. 58 (1991) 2924.